

Hydrodynamic Processes in Young Binary Systems as a Source of Cyclic Variations of Circumstellar Extinction

N.Ya. Sotnikova¹, V.P. Grinin^{1,2}

1 – Sobolev Astronomical Institute, St. Petersburg State University, Universitetskii pr. 28, Petrodvorets, St. Petersburg, 198504 Russia,

2 – Pulkovo Astronomical Observatory, Russian Academy of Sciences, Pulkovskoe sh. 65, St. Petersburg, 196140 Russia

Abstract

Hydrodynamic models of a young binary system accreting matter from the remnants of a protostellar cloud have been calculated by the SPH method. It is shown that periodic variations in column density in projection onto the primary component take place at low inclinations of the binary plane to the line of sight. They can result in periodic extinction variations. Three periodic components can exist in general case. The first component has a period equal to the orbital one and is attributable to the streams of matter penetrating into the inner regions of the binary. The second component has a period that is a factor of 5-8 longer than the orbital one and is related to the density waves generated in a circumbinary (CB) disk. The third, longest period is attributable to the precession of the inner asymmetric region of CB disk. The relationship between the amplitudes of these cycles depends on the model parameters as well as on the inclination and orientation of the binary in space. We show that at a dust-to-gas ratio of 1 : 100 and a mass extinction coefficient of $250 \text{ cm}^2 \text{ g}^{-1}$, the amplitude of the brightness variations of the primary component in the V-band can reach 1^m at a mass accretion rate onto the binary components of $10^{-8} M_{\odot} \text{ yr}^{-1}$ and a 10° inclination of the binary plane to the line of sight. We discuss possible applications of the model to pre-main-sequence stars.

Key words: *young binaries, accretion, hydrodynamics, variable extinction.*

INTRODUCTION

Binarity is widespread among stars, including young pre-main-sequence stars (see the review by Mathieu et al. 2000). Such stars still continue accreting matter from the remnants of a protostellar cloud. Numerical simulations by Artymowicz and Lubow (1994, 1996) of hydrodynamic processes in young binaries show that periodic gravitational perturbations and viscous forces produce a matter-free gap at the binary center into which two streams

¹email: nsot@astro.spbu.ru

of matter generally unequal in intensity from a circumbinary (CB) disk penetrate. These streams maintain the accretion activity of the binary components.

The simulations by Artymowicz and Lubow (1996) showed that the accretion rate in binaries with eccentric orbits depends on the orbital phase, reaching its maximum at the time of periastron passage. For this reason, in binaries whose components are cool young T Tauri stars (their luminosity depends sensitively on the accretion rate), periodic brightness variations in their components can take place. This prediction of the theory was confirmed by observations (Mathieu et al. 2000).

In this paper, we reproduce the Artymowicz–Lubow model by the SPH method and show that another type of cyclic photometric variability of a young binary due to periodic extinction variations on the line of sight is possible in this model. In contrast to periodic modulation of the accretion rate, periodic extinction variations can be observed in binaries with both elliptical and circular orbits, provided they are inclined at a small angle to the line of sight.

FORMULATION OF THE PROBLEM

Following Artymowicz and Lubow (1994, 1996), we assume that the circumbinary disk is coplanar with the binary. As in the papers of these authors, the hydrodynamic calculations presented below were performed by the smoothed particle hydrodynamics (SPH) method (Lucy 1977; Gingold and Monagan 1977) according to a scheme similar to that suggested by Hernquist and Katz (1989), but with a constant smoothing length of hydrodynamic quantities. No thermal balance was calculated. The system was assumed to be isothermal. The SPH implementation used was described in detail previously (Sotnikova 1996).

The Hydrodynamic Model

The mass of the gaseous disk was assumed to be negligible compared to the total mass of the stars in the binary. This allowed the disk self-gravity to be neglected. In the initial scheme, we assumed free boundary conditions, i.e., neglected the pressure at the boundary of the gas distribution. This approximation is justified if a flow of cold gas is modeled. During our calculations, it emerged that the presence of a free boundary led to a slow outward expansion of the disk, which deteriorated the statistics when the temporal variations in disk column density were determined. Therefore, the scheme was slightly modified: an artificial potential barrier on the far periphery of the disk was superimposed on the general gravitational field of the binary¹. The barrier parameters were chosen in such a way that, on the one hand, the disk dissipation was slowed down and, on the other hand, no significant distortions were introduced into the dynamics of density waves in the inner disk regions. Test calculations showed that introducing a barrier reduced the dissipation rate of the CB disk approximately twofold. In the models presented below, the dissipation is attributable mainly to mass accretion onto the binary components: through this process, the number of particles in the CB disk decreases approximately twofold after 600 binary revolutions. In the case without a barrier, the same result is obtained after 300 revolutions.

¹Note that a similar barrier was used with the same goal by Artymowicz and Lubow (1994, 1996).

The SPH equations of motion for particle i that represents an element of gas in are very similar to those described in (Hernquist and Katz 1989)

$$\frac{d\mathbf{v}_i}{dt} = -m \sum_j \left(\frac{2\sqrt{P_i P_j}}{\rho_i \rho_j} + Q_{ij} \right) \nabla_i W(\mathbf{r}_i - \mathbf{r}_j; h) - \nabla \varphi(\mathbf{r}_i),$$

where P_i, P_j, ρ_i, ρ_j are the pressure and density at the position \mathbf{r}_i and \mathbf{r}_j of particles i and j ; for the isothermal case under consideration, the equation of state is $P = c^2 \rho$, where c is the speed of sound; φ is a variable gravitational potential produced by the binary; m is the mass of the SPH particles (we considered equal-mass particles); W is the kernel for smoothing hydrodynamic quantities (it was chosen in the form of a spline; see Monaghan and Gingold 1983); h is the smoothing length.

The contribution from the artificial viscosity to the pressure gradient is described by the tensor Q_{ij} . There are various representations of Q_{ij} . We used its expression suggested by Monaghan and Gingold (1983). For advantages and disadvantages of this choice, see Hernquist and Katz (1989).

As in the papers by Artymowicz and Lubow, we took into account the contribution from the viscous terms in the cases where the SPH particles approached each other and recede from each other, i.e., in the form

$$Q_{ij} = (-\alpha c \mu_{ij} + \beta \mu_{ij}^2) / \rho_{ij},$$

where $\mu_{ij} = h(\mathbf{v}_i - \mathbf{v}_j) \cdot (\mathbf{r}_i - \mathbf{r}_j) / (r_{ij}^2 + \eta^2)$, $\rho_{ij} = (\rho_i + \rho_j) / 2$, $r_{ij} = |\mathbf{r}_i - \mathbf{r}_j|$, $\eta \simeq 0.1 h$. The parameters α and β are analogues of the viscosity coefficients in the Navier-Stokes equation. Following Artymowicz and Lubow (1994), we assumed for most of the models that $\alpha \simeq 1$ and $\beta = 0$.

The choice of parameter c , an isothermal speed of sound, is critical for our models. It defines the effective viscosity of the gaseous disk: $\nu \sim \alpha c h$. Following Artymowicz and Lubow (1994), we chose this parameter in units of the velocity of a test particle in a circular orbit with a radius equal to the semimajor axis of the binary moving around a point mass $m_1 + m_2$, where m_1 and m_2 are the masses of the binary components. The parameter c in these units was varied in the range from 0.01 to 0.08. Reducing the viscous properties of the disk reduced the contribution from hydrodynamic effects and the behavior of the system was similar to that of a celestial-mechanical system. Below, we call gaseous disks with $c \approx 0.01 - 0.02$ and $c = 0.05$ “cold” and “warm” CB disks, respectively.

The smoothing length was fixed at $h = 0.1a$, where a is the orbital semimajor axis of the secondary component. This allowed the hydrodynamic quantities to be smoothed over 40-60 neighboring particles at a typical number of particles $N \sim 60\,000$.

To integrate the SPH equations, we used the standard explicit leapfrog scheme; the time step dt was controlled by the Courant condition.

Initial Conditions and Binary Parameters

The number of test particles modeling the CB disk was chosen to be from 50 000 to 75 000. The particles were distributed in accordance with a surface density profile $\sim 1/r$. The radius of the matter-free gap at the initial time was taken to be $r_{\text{in}} = 2a$. After several binary revolutions, it virtually ceased to change and did not differ much from its initial value.

We put the outer boundary of the disk at the initial time at a distance $r_{\text{out}} = 5.8a$. Thus, we modeled more extended disks than Artymowicz and Lubow (1994). The periodic variations in gravitational potential produced no perturbations in this region of the gaseous disk and the existence of a boundary (in particular, the presence of a barrier) had no effect on the inner disk regions. The vertical particle distribution followed a barometric law.

At the initial time, the particles were placed in circular orbits around the center of mass of the binary with a Keplerian velocity corresponding to the orbital radius.

We varied the orbital eccentricity of the binary within the range from $e = 0$ to $e = 0.7$ and the component mass ratio $q = m_2/m_1$ within the range from 0.1 to 1.0. The evolution of the CB disk was traced on time scales up to 300 binary revolutions (in some cases, up to 600 revolutions). The orbital parameters of the binary in this time interval were assumed to be constant.

Determining the Column Density in the Disk

Simultaneously with the calculation of the dynamical evolution of the gaseous disk in the binary’s periodically varying potential, we determined the mass accretion rate from the disk onto both components. We assumed that if a particle fell into a region less than 0.3 of the radius of the corresponding Roche lobe, then it was captured by the star and contributed to the accretion rate. Subsequently, such particles were eliminated from our calculations. The derived accretion rates of test particles onto the binary components were then used to determine the particle mass when calculating the circumstellar extinction.

The particle column density was determined for various orbital phases and various inclinations of the line of sight to the binary plane. Let us denote the binary inclination to the line of sight by θ . To calculate the particle column density $n(\theta, t)$ as a function of time, we chose a column with a cross section $\sigma = 0.1a \times 0.2a$. Test calculations showed that the statistical fluctuations due to a small number of test particles in the column increase at lower values of σ , while the features on the t dependences of n are smoothed at higher values of σ .

RESULTS OF SIMULATIONS

As an example, Fig. 1 shows the particle distribution in the binary after 60 revolutions from the beginning of our calculation. The models with warm (a) and cold (b) disks are shown. The model parameters are: $e = 0.5$, $m_2 : m_1 = 0.7 : 2$, $c = 0.02$ for the cold disk; $c = 0.05$ for the warm disk.

In the model with a warm disk (Fig. 1a), we clearly see two streams of matter unequal in intensity from the CB disk, which feed the accretion disks of the binary components and which are extensions of the spiral density waves (the second stream is more pronounced at other intermediate orbital phases). The more intense stream accretes onto the less massive binary component. This peculiarity was first pointed out by Artymowicz and Lubow (1996) and, as the calculations by Bate and Bonnell (1997) showed, is obtained even in the models with a component mass ratio of 1 : 10. This is because the low-mass companion moves in its orbit not far from the inner boundary of the CB disk — the main reservoir of the matter that it “pulls” on itself, while the primary component of the binary is located near its center, in a matter-free zone. The characteristic size of this zone depends on orbital eccentricity e and component mass ratio q and is equal to $\approx (2 - 3)a$ (Artymowicz and Lubow (1994)). On the whole, the disk more likely resembles a wide ring.

In the “cold” model (Fig. 1b), the spiral pattern on the CB disk appears more fragmentary and is represented by several short remnants of the spiral density waves near the inner disk boundary. The accretion streams are less pronounced. The disk itself is geometrically thinner.

The Global Asymmetry of CB disk

We see from Figs. 1a and 1b that the distribution of matter in the CB disk is characterized by a global asymmetry seen in both projections of the binary. The asymmetry manifests itself particularly clearly in the inner disk region — the inner boundary of the ring has a noticeable eccentricity and its center is shifted relative to the binary center of mass. According to Lubow and Artymowicz (2000), such an eccentricity is the result of instability. It arises when there is a 3 : 1 resonance in the gaseous disk. This instability manifests itself even in binaries with circular orbits. For this instability to operate, the mass ratio of components q must be

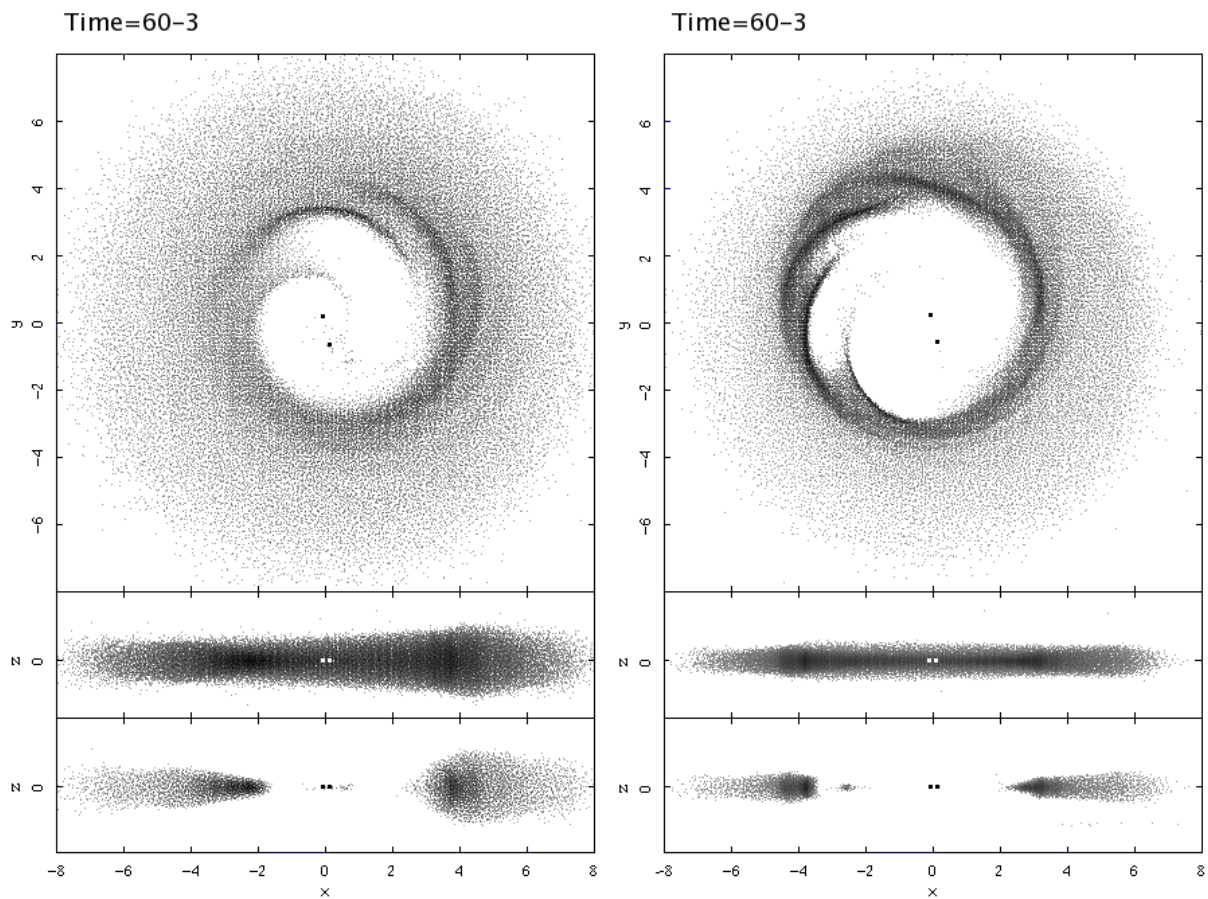


Figure 1: Binary models with warm (a) and cold (b) disks and a low-mass ($m_2 : m_1 = 0.7 : 2$) secondary component in an eccentric ($e = 0.5$) orbit. The figure shows the following: view from the pole (upper panels), projection onto the xz plane (middle panels), and section (lower panels) passing through the center of mass in this plane. The binary is displayed in revolution 61 at phase $3/8$. The strength of the image blackening corresponds to the logarithm of the particle number per pixel.

greater than 0.2. On the other hand, the component masses must differ, q cannot be close to unity, or the instability will be damped by viscosity.

Additional effects arise in the case of eccentric orbits. The presence of an one-armed bar potential with $(m, l) = (1, 0)$ results in lopsided structure of a disk. The disk disturbance produced by a variable gravitational potential follows the apsidal motion of the binary. The disk eccentricity varies periodically and the rate of these variations depends on the angle between the major axes of the binary orbit and the elliptical disk itself. The effects of disk precession due to the quadrupole moment from the binary are added to this. The precession rate is low and the entire eccentric disk turns in a time interval that is hundreds of times longer than the orbital period.

If we look at the disk edge-on, then its significant asymmetry is also noticeable in the vertical direction: on the one side, it is considerably thicker than on the other side (Fig. 1, central panels). We are probably the first to point out this peculiarity of CB disks. The part of the disk whose inner boundary is located farther from the center of mass turns out to be thicker. The thickening may be caused by a weakening of the gravitational forces from the binary, which is known to result in an increase in the geometrical thickness of the disk in an external gravitational field.

Figure 2 demonstrates the vertical asymmetry and the overall turn of the warm disk on time scales of the order of one precession period ($\approx 200 P$, where P is the orbital period of the binary). The parameters of the presented model are $e = 0.5$, $m_2 : m_1 = 1 : 2$, and $c = 0.05$. As we will show below, the existence of a global asymmetry in the CB disk is one of the reasons why the optical properties of a young binary at low inclinations to the line of sight depend significantly on its orientation in space.

The global asymmetry in the cold disk on time scales of several hundred binary revolutions is more pronounced than that in the warm disk. This is particularly clearly seen if we look at the disk edge-on. Its precession time is approximately twice that for the warm disk. Figure 3 shows the projections of the cold disk onto the xz and yz planes at various times. In a time of about 200 orbital periods, the disk in the yz projection turns approximately through 180° , while in the “warm” model the CB disk made an almost complete turn. The CB disk precession and asymmetry, which is particularly clearly seen in the vertical direction, are common properties of such disks and take place not only in the models with eccentric orbits, but also in those with circular orbits. Moreover, we found no significant dependence of the precession period on eccentricity.

The Behavior of the Column Density

Our calculations showed that the particle column density in binaries with elliptical orbits toward the primary component depends not only on the orbital phase and the orbital inclination to the line of sight θ , but also on the orientation of the orbit relative to the observer. Figure 4 shows the behavior of the column density $n(\theta, t)$ for two angles, $\theta = 0^\circ$ and $\theta = 10^\circ$, and one of the orbital orientations relative to the observer at which the azimuth angle between the direction from the primary component to the apoastron of the secondary star and the observer’s direction is zero. In this case, the orbital apoastron of the secondary component lies between the observer and the primary component.

We see from Fig. 4 that two cycles are present in the column density variations. One of them has a period equal to the orbital period. Its amplitude is larger in the case with an

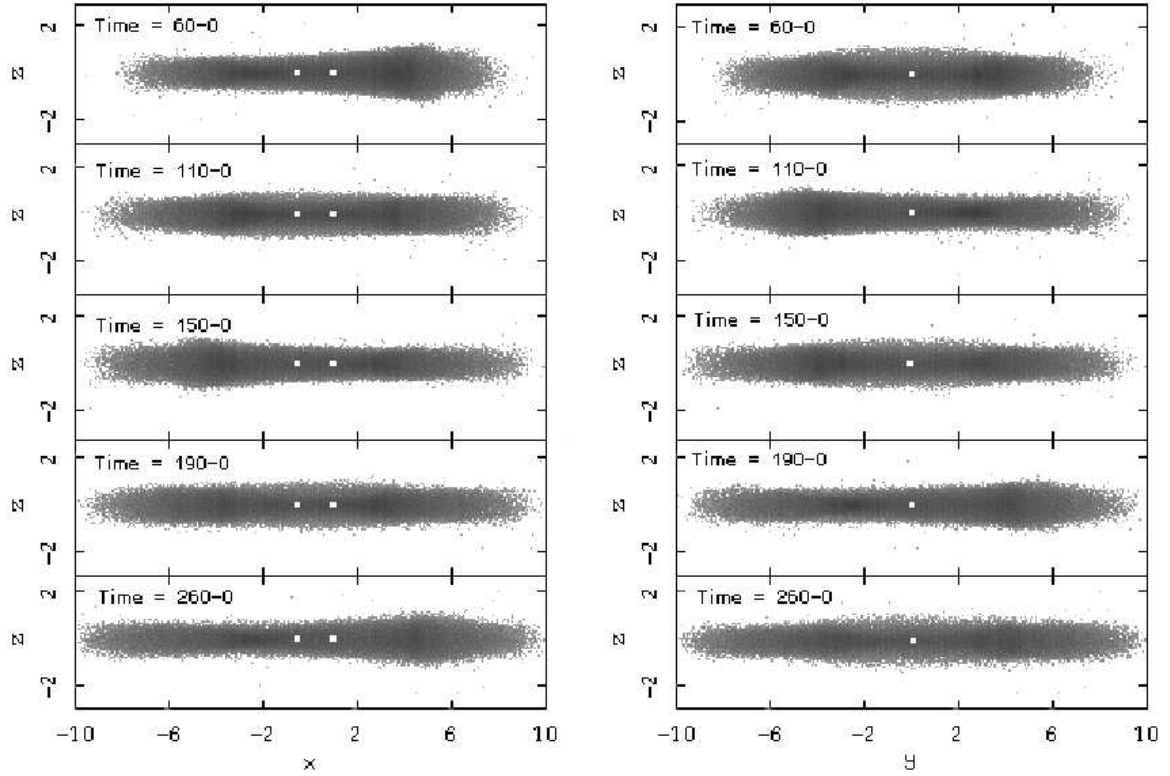


Figure 2: Precession of the warm disk in projections onto the xz and yz planes at various times. The time is given in units of the orbital period. The model parameters are $m_2 : m_1 = 1 : 2$ and $e = 0.5$. The strength of the image blackening corresponds to the logarithm of the particle number per pixel.

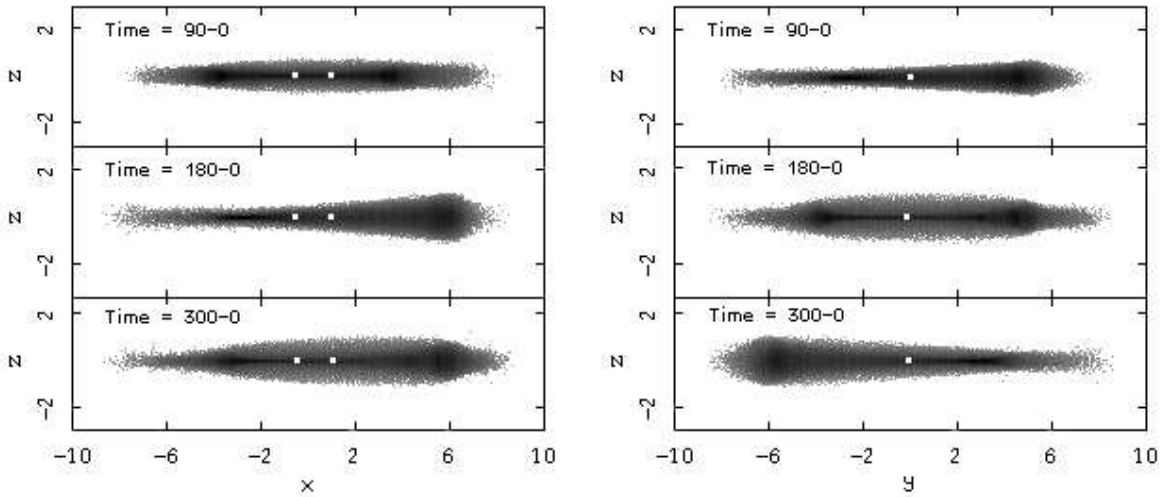


Figure 3: Same as Figure 2 for the cold disk. The binary parameters are $m_2 : m_1 = 0.7 : 2$ and $e = 0.5$. The strength of the image blackening corresponds to the logarithm of the particle number per pixel.

inclination of 10° and is barely noticeable in the case with $\theta = 0^\circ$. This cycle originates from the streams of matter accreting onto the binary components and periodically crossing the line of sight. The second component in the dependence on model parameters has a period that is approximately a factor of 6-8 longer than the orbital one. It owes its origin to the motion of density waves in the inner CB disk region. Comparison of the solutions obtained at the same θ , but at different binary orientations relative to the observer shows that the relationship between these two components depends sensitively on the observer's direction. This dependence originates from the global CB disk asymmetry discussed above. The slow secular turn of an asymmetric disk changes the relationship between the amplitudes of the short and longer periods of the column density variations at the same orbital inclination.

Figures 5 and 6 show the column density variations on a long time scale (300 orbital periods) for four orbital orientations relative to the observer corresponding to azimuth angles ϕ equal to 0° , 90° , 180° , and 270° (the angles are measured from the direction of the apoastron of the secondary in the direction opposite to its orbital motion). As has already been noted above, in the first of these cases, the orbital apoastron of the secondary component lies between the observer and the primary component. In the third case, the binary is viewed from the periastron. In addition, for each of the four listed cases, we considered two orbital inclinations: $\theta = 0^\circ$ (Figs. 5a and 6a) and $\theta = 10^\circ$ (Figs. 5b and 6b).

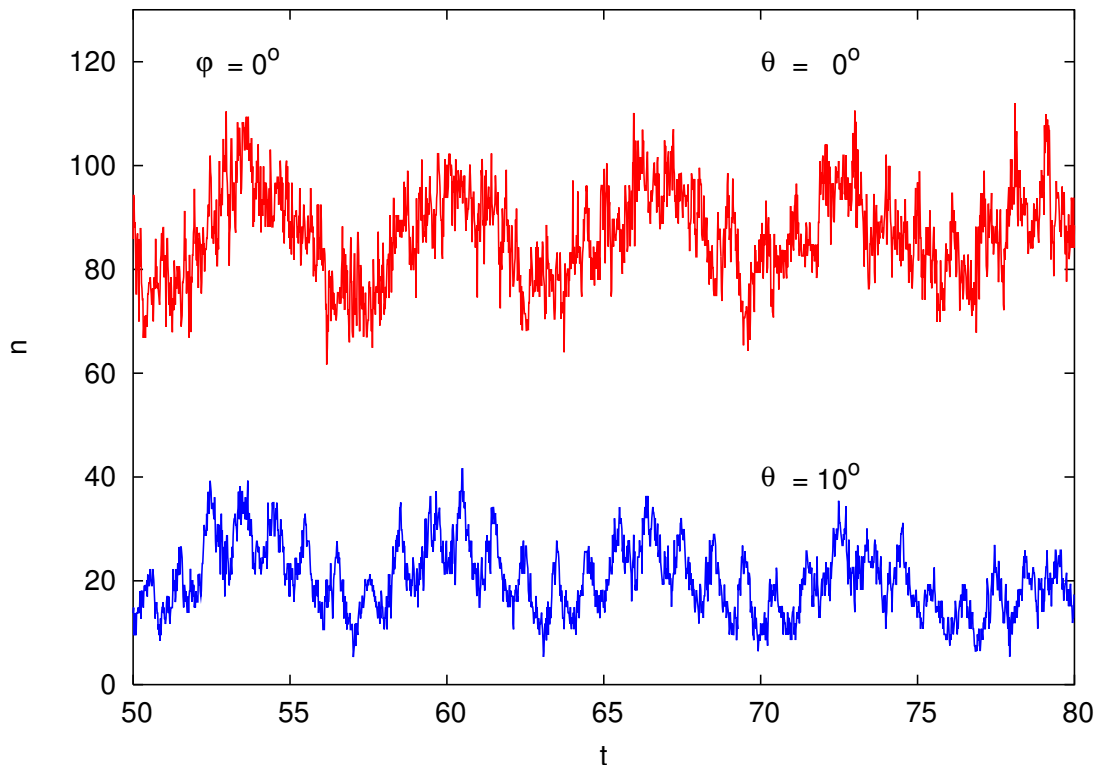


Figure 4: Variations in column density $n(\theta, t)$ for two orbital inclinations with respect to the observer: $\theta = 0^\circ$ (solid line) and $\theta = 10^\circ$ (dotted line). The orbit is turned to the observer in such a way that the apoastron of the secondary component lies between the observer and the primary star. The model parameters are $m_2 : m_1 = 1 : 2$, $e = 0.5$, the warm disk. The time is given in units of the orbital period.

Slow CB disk precession produces a long-period modulation of $n(\theta, t)$. As a result, apart from the two periodic components discussed above, a secular period is also present in the column density variations with time. There is also a slow decrease in column density with time common to all models that is attributable to gradual CB disk dissipation due to mass accretion onto the binary components. The secular period of the column density variations is equal to the precession period of the inner region of an asymmetric CB disk and is $\sim 200 P$ for the models presented in Fig. 2. In observations at $\theta = 0^\circ$, the line of sight passes through different parts of the asymmetric gaseous ring. As a result, the values of n in the global modulation curve for the same time, but for different orbital orientations relative to the observer are different (Figs. 5a and 6a). In the directions (along the line of sight) where the disk is more extended, the column density is higher.

In observations at $\theta = 10^\circ$, the picture is significantly different (Figs. 5b and 6b). Over fairly long time intervals, the column density decreases almost to zero. At these times, the thin side of the disk is turned to the observer and the line of sight hardly touches it. The small n variations in these time intervals stem from the fact that the line of sight periodically crosses the stream of matter directed to the secondary component. Thus, because of the CB disk precession, a young binary whose equatorial plane is slightly inclined to the line of sight can be observable in certain time intervals and may turn out to be completely occulted from the observer by its own CB disk after a lapse of time and this occultation can last very long.

In general case, the three different (in duration) periods of the column density variations manifest themselves as follows. The secular (precession) period manifests itself clearly in the models with both circular and eccentric orbits. A decrease in viscosity causes an increase in precession period (for the models with $e = 0.5$ and $m_2 : m_1 = 0.7 : 2$, the secular period for the cold disk increases by almost a factor of 2 compared to the warm model and is $\sim 400 P$). For binaries with high eccentricities ($e = 0.5, 0.7$), the period related to the motion of density waves at the inner disk boundary (5-8 orbital periods, depending on the model parameters) is superimposed on the secular period. This second period shows up particularly clearly at the maxima of the secular $n(\theta, t)$ modulation amplitudes (Figs. 5 and 6). In this case, its amplitude in “cold” binaries is smaller than that in “warm” ones.

Since apart from gas, there is also dust in the streams of matter penetrating from the CB disk into the inner region of the binary, the periodic variations in column density will be accompanied by periodic extinction variations. Taking the standard dust-to-gas ratio for the model considered above to be 1 : 100 and the mass extinction coefficient to be $250 \text{ cm}^2 \text{ g}^{-1}$, we estimated the photometric effect due to the periodic column density variations. The amplitude of the V-band brightness variations in the primary component at a 10° inclination of the binary plane to the line of sight turned out to be about 1^m at an accretion rate of $10^{-8} M_\odot \text{ yr}^{-1}$. In binaries with a higher accretion rate, an appreciable (in amplitude) cyclic activity can be observed at a higher binary inclination to the line of sight.

CONCLUSIONS

The results of our hydrodynamic calculations presented above show that cyclic variations in the column density of matter accreting onto the binary components can take place in young binaries inclined at a small angle to the line of sight. The fundamental period of these variations is equal to the orbital one and is attributable to the streams of matter in the inner parts of the binary that are periodically projected onto the primary component. The second

period is produced by the motion of spiral density waves in the CB disk and is a factor of 5-8 longer than the orbital one. At low inclinations of the binary, both $n(\theta, t)$ oscillation modes can be present simultaneously. The relationship between them depends both on the inclination of the binary plane and on its orientation in space.

Apart from these two cycles, there is also a secular cycle with a duration of the order of several hundred orbital periods in the behavior of the column density. This cycle is attributable to the precession of the inner parts of an asymmetric CB disk. The lower the viscosity, the longer its duration. The characteristics of the two shorter cycles (primarily their amplitude) depend significantly on the phase of the secular cycle (Figs. 5 and 6). Note also that the existence of a global asymmetry in the distribution of matter in the inner CB disk region must be taken into account when the intrinsic polarization in young binary stars is modeled.

The periodic variations in column density can be accompanied by noticeable extinction and brightness variations in the binary. Such variations are observed in UX Ori stars (Shevchenko et al. 1993; Grinin et al. 1998; Rostopchina et al. 2000; Bertout 2000). The brightness of these stars is known to undergo great variations attributable to extinction variations in circumstellar disks inclined at a small angle to the line of sight (see the review by Grinin (2000) and references therein). Both “rapid” variability on time scales of the order of several days with an irregular (unpredictable) pattern and slow variability on a time scale from several to twenty years or more are observed. In a number of stars, the slow component is cyclic in pattern. In two cases, SV Cep (Rostopchina et al. 2000) and CQ Tau (Shakhovskoi et al. 2005), the cyclic activity is described by two oscillation modes with a period ratio close to that obtained above (5-8). Therefore, the idea that the cyclic activity of UX Ori stars can be the result of their latent binarity seems quite plausible.

Other objects of application of the theory considered above can be such young binaries with abnormally long occultations as KH 15D (Winn et al. 2006), H 187 (Grinin et al. 2006; Nordhagen et al. 2006), and GW Ori (Shevchenko et al. 1998). There are the reasons to assume that the equatorial planes of these binaries are inclined at a small angle to the line of sight and, hence, periodic variations in column density can take place. We are going to return to a discussion of these questions in the next papers.

ACKNOWLEDGMENTS

We thank Pawel Artymowicz for a helpful discussion of the questions touched upon in the paper. This work was performed as part of the “Origin and Evolution of Stars and Galaxies” Program of the Presidium of the Russian Academy of Sciences under support of INTAS grant no. 03-51-6311 and grant no. NSh-8542.2006.2.

REFERENCES

1. P. Artymowicz and S. H. Lubow, *Astrophys. J.* **421**, 651 (1994).
2. P. Artymowicz and S. H. Lubow, *Astrophys. J.* **467**, L77 (1996).
3. M. R. Bate and I. A. Bonnell, *Mon. Not. R. Astron. Soc.* **285**, 33 (1997).
4. C. Bertout, *Astron. Astrophys.* **363**, 984 (2000).
5. R. A. Gingold and J. J. Monagan, *Mon. Not. R. Astron. Soc.* **181**, 375 (1977).
6. V. P. Grinin, *Astron. Soc. Pac. Conf. Ser.* **219**, 216 (2000).

7. V. P. Grinin, O. Yu. Barsunova, S. G. Sergeev, et al., *Pis'ma Astron. Zh.* **32**, 918 (2006) [*Astron. Lett.* **32**, 827 (2006)].
8. V. P. Grinin, A. N. Rostopchina, and D. N. Shakhovskoi, *Astron. Lett.* **24**, 802 (1998).
9. L. Hernquist and N. Katz, *Astrophys. J., Suppl. Ser.* **70**, 419 (1989).
10. S. H. Lubow and P. Artymowicz, *Protostars and Planets IV*, Ed. by V. Mannings, A. Boss, and S. S. Russell (Univ. Arizona Press, Tucson, 2000), p.731.
11. L. B. Lucy, *Astron. J.* **82**, 1013 (1977).
12. R. D. Mathieu, F. C. Adams, and D. W. Latham, *Astron. J.* **101**, 2184 (1991).
13. R. D. Mathieu, A. M. Ghez, E. K. N. Jensen, and M. Simon, *Protostars and Planets IV*, Ed. by V. Mannings, A. Boss, and S. S. Russell (Univ. Arizona Press, Tucson, 2000), p. 559.
14. J. J. Monaghan and R. A. Gingold, *J. Comp. Phys.* **52**, 374 (1983).
15. S. Nordhagen, B. Herbst, E. C. Williams, and E. Semkov, astro-ph/0606501 (2006).
16. A. N. Rostopchina, V. P. Grinin, D. N. Shakhovskoi, et al., *Astron. Zh.* **77**, 420 (2000) [*Astron. Rep.* **44**, 365 (2000)].
17. D. N. Shakhovskoi, V. P. Grinin, and A. N. Rostopchina, *Astrofizika* **48**, 165 (2005) [*Astrophys.* **48**, 135 (2005)].
18. V. S. Shevchenko, K. N. Grankin, M. A. Ibragimov, et al., *Astrophys. Space Sci.* **202**, 121 (1993).
19. V. S. Shevchenko, K. N. Grankin, S. Yu. Mel'nikov, and S. A. Lamzin, *Pis'ma Astron. Zh.* **24**, 614 (1998) [*Astron. Lett.* **24**, 528 (1998)].
20. N. Ya. Sotnikova, *Astrofizika* **39**, 259 (1996) [*Astrophys.* **39**, 141 (1996)].
21. J. N. Winn, C. M. Hamilton, W. J. Herbst, et al., *Astrophys. J.* **644**, 510 (2006).

Translated by V. Astakhov

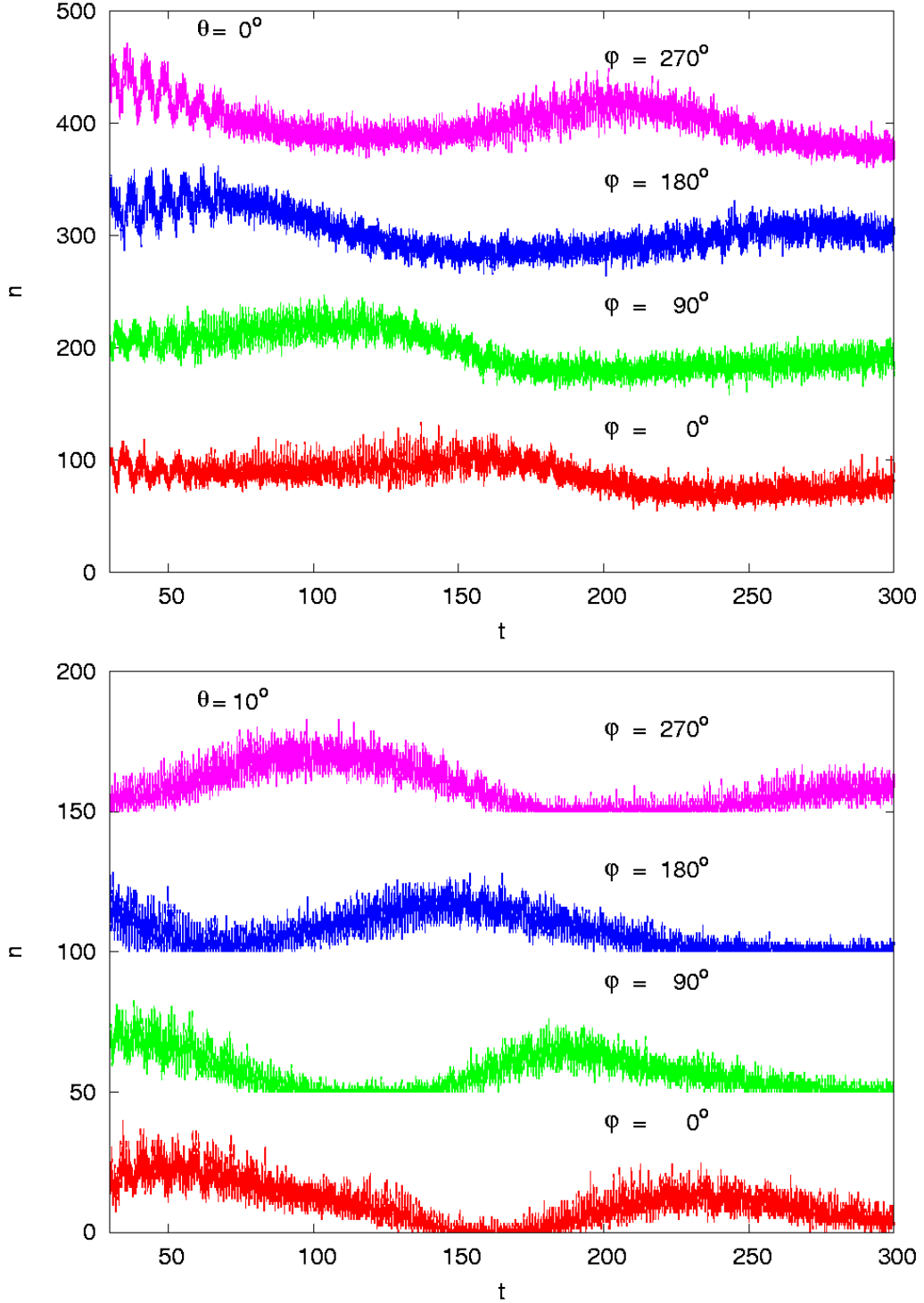


Figure 5: Variations in column density $n(\theta, t)$ for two orbital inclinations with respect to the observer: (a) $\theta = 0^\circ$ and (b) $\theta = 10^\circ$. The variations in column density with time are shown in each plot for one of the four orbital orientations with respect to the observer (from the bottom upward: the angles ϕ between the directions of the apoastron of the secondary component and the observer as viewed from the primary star are, respectively, 0° , 90° , 180° , and 270°). For convenience, the upper and lower plots were displaced with respect to one another by 100 and 50 units along the y axis, respectively. The model parameters are $m_2 : m_1 = 0.7 : 2$ and $e = 0.5$, the warm CB disk. The time is given in units of the orbital period.

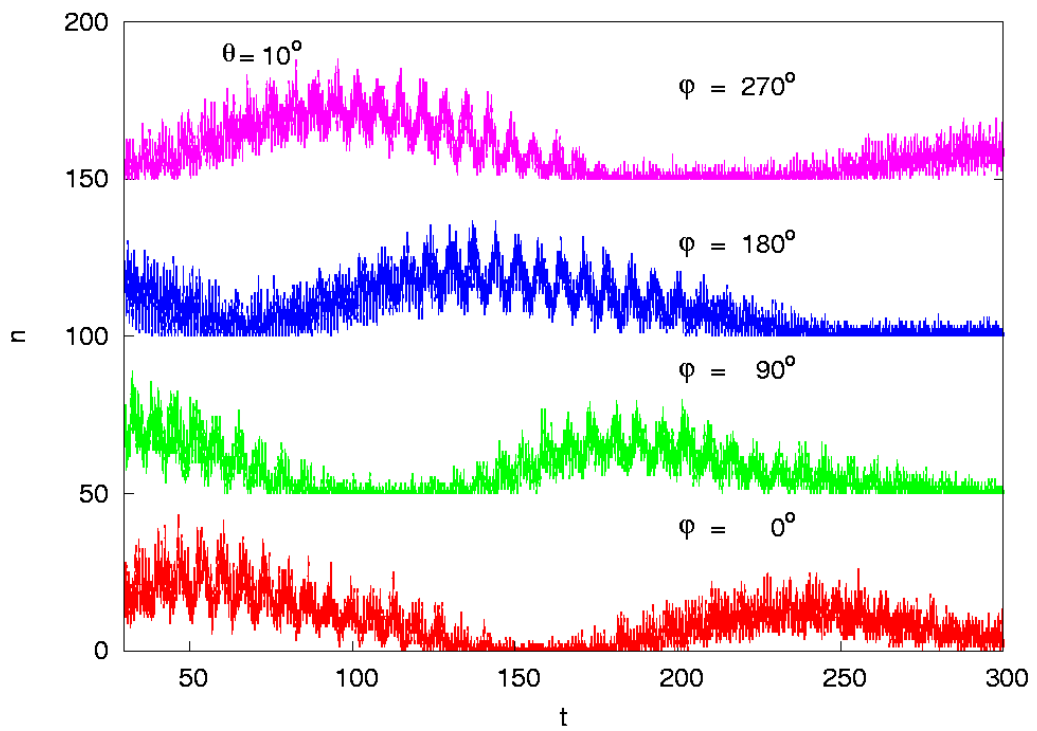
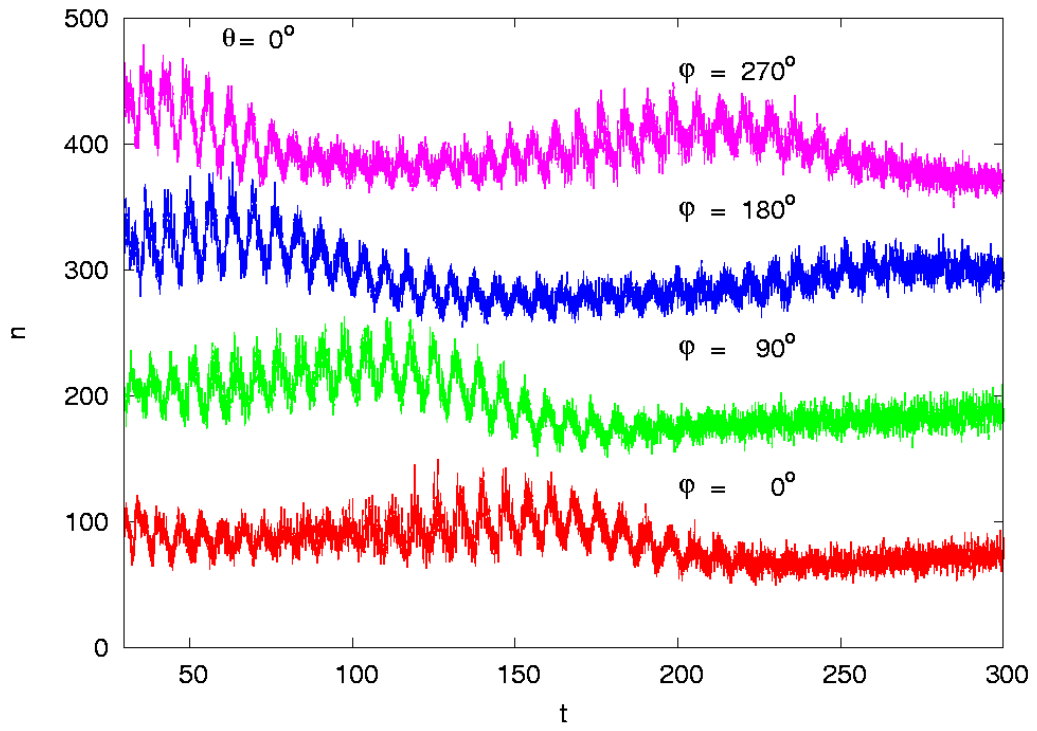


Figure 6: Same as Figure 5 for $m_2 : m_1 = 1 : 2$.